Bioscene

Bioscene
Volume- 22 Number- 04
ISSN: 1539-2422 (P) 2055-1583 (O)
www.explorebioscene.com

Computational Insights into Neem-Derived Proteins Targeting Cyclin-Dependent Kinases and Tubulin for Anticancer Therapy

Mohammed Al Saiqali[1] , Ayla Sanjay[2] and Chand Pasha [2]

1.Coordinator of Research and Innovation, Anwarul Uloom College, New Mallepally, Hyderabad, Telangana state, India

2. Department of Microbiology, Nizam College, Osmania University, Hyderabad, India

Corresponding Author: **Chand Pasha**

Abstract: Azadirachtaindica (Neem) is a medicinal plant known for its anticancer, antimicrobial, and antioxidant properties. This study evaluated five Neem-derived proteins Cytochrome P450 (full and partial forms), Squalene Epoxidase 1, Cytochrome f (chloroplast), and a Putative LOV Domain-Containing Protein for potential anticancer activity using in silico methods. Proteins were isolated and characterized through SDS-PAGE and MALDI-TOF/TOF mass spectrometry, followed by 3D structural modelling via SWISS-MODEL. Model validation using PROCHECK assessed Ramachandran plots, rotamer outliers, and clash scores to ensure stereochemical accuracy. Molecular docking was performed against two cancer-associated targets, Cyclin-Dependent Kinases (CDKs) and tubulin, using ZDOCK 3.0.2. The Putative LOV Domain-Containing Protein showed the strongest affinity for CDK, forming 43 amino acid interactions with a binding energy of −45,752.6 kJ/mol. Residues such as THR14, LYS34, GLU15, ASP14, HIS162, SER208, GLU209, PRO62, TYR7, TYR8, TYR248, ALA115, ASN245, MET324, and LEU237 contributed to extensive hydrogen bonding and electrostatic networks, suggesting effective suppression of CDK-mediated cell-cycle progression. Squalene Epoxidase 1 displayed dual-target activity, interacting with 31 CDK residues (−69,219.0 kJ/mol) and 41 tubulin residues (−53,204.0 kJ/mol). Key contacts including PRO40, HIS205, GLY206, ARG71, SER230, TYR66, GLU70, and ARG73 indicate potential disruption of kinase signalling and microtubule polymerization. Cytochrome P450 (full length) also showed high affinity toward tubulin, forming 41 interactions (−51,616.0 kJ/mol) primarily through ASN424, ILE788, GLU196, SER795, HIS704, VAL790, TYR867, and ARG868. All complexes demonstrated stability, supported by favourable energy landscapes and low RMSD values (1.2–2.0 Å). Overall, the Putative LOV Domain-Containing Protein, Squalene Epoxidase 1, and Cytochrome P450 emerged as promising candidates for modulating CDK and tubulin activity. These results highlight the potential of Neem-derived proteins as plant-based anticancer agents and provide a foundation for sustainable cancer therapeutics.

Keywords: Azadirachtaindica protein, Cytochrome P450, Cyclin-Dependent Kinase (CDK) inhibition, Tubulin polymerization inhibition, Molecular docking, anticancer therapeutics

Introduction:

Small peptides widely exist in nature and have been found to possess a variety of biological functions. These functions include immune regulation, angiogenesis, wound healing, and antitumor activity (Mookherjee et al., 2020; Roudi et al., 2017; Zhang et al., 2016; Pfalzgraff et al., 2018). The treatment of cancer has traditionally relied on chemotherapy and radiotherapy. However, their prolonged use often results in drug resistance, off-target toxicity, and limited efficacy because of their single-pathway mechanisms. In contrast, anticancer peptides (ACPs) exert their effects through multi-target actions. These actions include membrane disruption, induction of apoptosis, inhibition of angiogenesis, and modulation of oncogenic signaling pathways. These multifaceted mechanisms enable ACPs to act selectively against cancer cells while sparing normal tissues. This selectivity reduces the likelihood of resistance development. Consequently, ACPs are emerging as a promising class of therapeutic agents and a viable alternative to conventional chemotherapeutic drugs for combating resistant and aggressive cancers (Hoskin & Ramamoorthy, 2008; Hancock et al., 2021).Azadirachta indica was recognized by several medicinal systems like Ayurveda, Siddha, Unani, Yoga, Naturopathy, and Homeopathy. The tree is highly valued for its insecticidal and pharmaceutical qualities, which come from various highly valuable compounds like limonoids (like azadirachtin, gedunin, and nimbolide), alkaloids (such as nimbin and nimbidin), flavonoids (including quercetin), tannins, and terpenoids found in its different parts.The extracts of seeds, leaves, flowers, and fruits of neem have consistently shown chemopreventive and antitumor effects in different types of cancer (Hao et al., 2014). Neem has demonstrated potent antifungal, antibacterial, anti-helminthic, and anticancer activities across various extracts and phytoconstituents (Sonali Ray et al., 2022 & Mohideen M et al., 2022). Studies have shown that Neem-derived compounds such as nimbidin, azadirachtin, and nimbolide exhibit inhibitory effects against fungal pathogens like Candida albicans, Aspergillus niger, and dermatophytes, as well as helminths including Pheretimaposthuma and Tubifex. Recent advances in plant-derived protein therapeutics have demonstrated promising avenues for combating AMR (Al Saiqali et al., 2021 & Rout et al., 2024).Cancer remains a major global health challenge with an increasing burden, projected to cause 35 million new cases annually by 2050, (Bray et al., 2018 & Boyle et al., 2008).

By utilizing the inherent bioactivity of Neem proteins and validating their interactions through computational pipelines, this work contributes to the development of sustainable, plant-based therapeutics that can complement or replace conventional cancer inhibitors. This integrative approach not only reinforces the therapeutic versatility of Neem-derived proteins but also aligns with the growing demand for sustainable, plant-based solutions to counteract antibiotic-resistant infections. Many new chemical structures were designed and synthesized regarding cancer's biological targets, such as cyclin-dependent kinase (CDK), epidermal growth factor (EGF), Ras, and tubulin proteins(Patrick et

al., 2013; Hawash et al., 2019).Tubulin is considered one of the most useful and strategic molecular targets for antitumor drugs (Singh H et al., 2016). Interruption of a deregulated cell cycle, as a consequence of overactivation of a Cdk, has been accepted as a strategy for treatment of cancer (Helal et al., 2004; Soni et al., 2001; Hörmann et al., 2001; Jenkins et al., 2008). The natural pigment fascaplysin has a range of interesting properties (Varinska et al., 2017). It is capable of suppressing the proliferation of mouse leukaemia cells and is a potent inhibitor of cyclin-dependent kinase 4 (CDK4), causing cell cycle arrest at the G1 phase of the cell cycle in both normal and tumour cell lines. The overarching goal is to identify candidate proteins capable of effectively binding, blocking, and inhibiting these key oncogenic regulators, thereby providing predictive insights that could guide the development of novel plant-based anticancer therapeutics.

2. Materials and Methods:

2.1 Sample collection

Young fresh leaves of *Neem* were collected from the Nizam College campus (Hyderabad, India) in August 2024. The plant material was taxonomically identified and authenticated by Dr. Vijaya Bhaskar Reddy, Professor, Department of Botany, Osmania University (O.U.). A voucher specimen (No. NC-1-Aug., 2024) was prepared and deposited in the O.U. Herbarium for future reference. Prior to extraction, the leaves were thoroughly rinsed with distilled water to remove surface debris and potential contaminants. The cleaned samples were subsequently air-dried at a controlled temperature of 25 °C under shade to preserve their biochemical integrity and prevent degradation of heat-sensitive compounds.

2.2 Protein extraction and purification

Dried Neem leaf powder (3 g) was used for protein extraction. The powdered material was homogenized in an Tris HCl extraction buffer pH7.4 and subjected to continuous agitation on a shaker at 4 °C for 1 hour to ensure thorough solubilization of cellular proteins. The homogenate was then centrifuged at 12,000 rpm for 25 minutes under refrigerated conditions, and the resulting supernatant was carefully collected for subsequent processing. Protein precipitation was achieved by adding 15% trichloroacetic acid (TCA) in acetone at a 4:1 (v/v) ratio, supplemented with 0.07% β - mercaptoethanol (β-ME). The mixture was incubated at −20 °C overnight to facilitate complete precipitation. The precipitated proteins were recovered by centrifugation at 12,000 rpm for 25 minutes at 4 °C. The resulting protein pellets were washed three times with 90% chilled acetone containing β-ME to remove residual TCA and other contaminants, followed by centrifugation after each wash under the same conditions. Following the final wash, the pellets were air-dried under aseptic conditions to allow complete evaporation of residual acetone. The purified protein extracts were subsequently stored at −80 °C until further biochemical and in silico analyses.

2.3 SDS Page and MALDI/TOF-TOF Mass Spectrometry identification

Protein samples were solubilized and subjected to electrophoretic separation on a 15% SDS–polyacrylamide gel electrophoresis (SDS-PAGE) system alongside a molecular weight marker for reference. Following electrophoresis, the gel was rinsed thoroughly with deionized water, and low–molecular-weight protein bands of interest were excised aseptically using a sterile surgical blade for downstream analysis by MALDI-TOF/TOF mass spectrometry. Excised gel fragments were destained using a 50% (v/v) acetonitrile–water solution containing 25 mM ammonium bicarbonate, followed by buffer exchange and dehydration with 100% acetonitrile. Disulfide bonds were reduced by incubating the gel plugs in 100 mM dithiothreitol (DTT) at 56 °C for 1 hour, and alkylation was performed with 250 mM iodoacetamide in the dark at 25 °C for 45 minutes. Proteolytic digestion was carried out using in-gel trypsin treatment, and the resulting tryptic peptides were extracted with 0.1% trifluoroacetic acid (TFA), vacuum-dried, and reconstituted in 10 µL of TA buffer. A 1.5 µL aliquot of each peptide sample was mixed with an equal volume of α-cyano-4-hydroxycinnamic acid (CHCA) matrix and spotted onto a MALDI target plate for analysis. Mass spectra were acquired using a MALDI-TOF/TOF mass spectrometer, and peptide mass fingerprints were matched against the Swiss-Prot and NCBI protein databases for protein identification. Sequence homology and molecular identity were further confirmed using the Basic Local Alignment Search Tool (BLASTp) against the neem protein database to validate the identified proteins.

2.4 Selection of Neem Proteins

Five Neem proteins were selected based on protein extraction and MALDI TOF/TOF spectrometry analysis. Their sequences were retrieved from the UniProt neem database. To evaluate anticancer interactions, twocancer target proteins were chosen: CDK and tubulin. These cancer targets represent key mechanisms as Cyclin-dependent kinases (CDKs) and tubulin involved in cell cycle regulation and identified to be overexpressed in many cancers.

2.5 Neem and Bacterial Proteins Structure Homology Modeling and Validation

The three-dimensional (3D) structures of the selected *Azadirachta indica* (Neem) proteins were generated using the SWISS-MODEL server (Waterhouse et al., 2018), which employs a template-based homology modeling approach. For each Neem protein, suitable structural templates were identified by performing BLASTp searches against the Protein Data Bank (PDB) to determine homologous proteins with known crystal structures. Templates exhibiting high sequence identity (>40%) and model coverage exceeding 90% were prioritized to ensure that the majority of the target protein sequence was accurately represented in the resulting model.The selected templates were used to construct preliminary 3D models, which were subsequently refined and validated within the SWISS-MODEL framework. Validation included assessment of stereochemical quality and backbone conformation using PROCHECK, Ramachandran plot analysis, and

rotamer evaluation, ensuring that all modeled structures exhibited favorable geometrical parameters suitable for downstream molecular docking and interaction analyses.

2.6 Molecular Docking Studies

Molecular docking studies were performed to predict and evaluate the interaction potential between the modelled Neem proteins and the selected cancer-associated targets, Cyclin-Dependent Kinases (CDKs) and tubulin. Docking simulations were carried out using ZDOCK version 3.0.2 (Pierce BG et al., 2014), a rigid-body docking algorithm that employs a Fast Fourier Transform (FFT)-based search to explore all possible binding orientations between receptor and ligand proteins. The receptor structures of CDK (Accession No. NP_001307847.1) and tubulin(Accession No. VDK36218.1) were retrieved from the Protein Data Bank (PDB). All receptor molecules were pre-processed by removing crystallographic water molecules, ligands, and ions, followed by energy minimization using Swiss-PDB Viewer (SPDBV_4.10_PC) to relieve steric clashes and optimize side-chain conformations. The five Neem-derived proteins—Cytochrome P450 (full and partial), Squalene Epoxidase 1, Cytochrome f (chloroplast), and Putative LOV Domain-Containing Protein—were used as ligands. Their energy-minimized three-dimensional structures were generated via SWISS-MODEL and validated using PROCHECK to ensure stereochemical integrity. Docking was performed on a grid-based rotational search covering the entire receptor surface, evaluating over 54,000 rotational conformations per docking run. The complexes were scored based on shape complementarity, electrostatic potential, and desolvation free energy. The top ten docking poses were ranked according to their ZDOCK score and further refined through interface energy minimization using SPDBV to improve binding accuracy. Protein–protein interaction interfaces were visualized and analysed using SPDBV and Discovery Studio Visualizer (BIOVIA, 2021). The number of hydrogen bonds, hydrophobic interactions, and salt bridges were quantified, and the binding energy for each complex was computed using the default force-field parameters within ZDOCK. The amino acid residues involved in hydrogen bonding and van der Waals interactions were identified and mapped for both CDK and tubulin complexes to determine key stabilizing contacts. The resulting docking scores, energy values, and interacting residues were used to assess the binding strength and stability of Neem-derived proteins toward the selected cancer targets, thereby identifying the most promising candidates for downstream *in vitro* validation.

2.7 Energy calculation and Energy interpretation

The binding energies of the docked complexes between A.indica proteins and the cancer targets Cyclin-Dependent Kinases (CDKs) and tubulin were calculated using the default scoring and force-field functions implemented in ZDOCK 3.0.2(Pierce BG et al., 2014). The total binding energy (E_{binding})

was computed as the sum of van der Waals, electrostatic, and desolvation contributions:

Ebinding=EvdW+Eelectrostatic+EdesolvationE {binding} = E {vdW} + E{electrostatic} + E{desolvation}Ebinding=EvdW+Eelectrostatic+Edesolvation

Following docking, each complex was subjected to energy minimization using Swiss-PDB Viewer (SPDBV_4.10_PC) to optimize side-chain conformations and eliminate steric clashes. The refined complexes were further analyzed to assess interaction energy, interface area, and stability.

2.8Visualization and Interaction Mapping

Visualization and interaction mapping were performed to characterize the molecular interfaces between the*indica* (Neem) proteins and the cancer targets Cyclin-Dependent Kinases (CDKs)andtubulin**.** The top-ranked docked complexes from ZDOCK 3.0.2 were analyzed using Swiss-PDB Viewer (SPDBV_4.10_PC) **and** BIOVIA DiscoveryStudio Visualizer (2021).Hydrogen bonds, hydrophobic interactions, and electrostatic contacts were identified using the *Interaction Analysis* tool in Discovery Studio, with hydrogen bond distances defined at <3.5 Å. The electrostatic surface potential and solvent-accessible surface area (SASA) were computed to assess charge complementarity and interface stability (Mitternacht S et al.,2016).

3. Results

3.1 SDS-PAGE-MALDI TOF Analysis and Structural Modeling of Neem Proteins:

The amino acids sequences of the analyzed proteins were obtained by MALDI TOF Analysis. These sequences were collected and further submitted for in silico studies to predict the protein structure.MALDI-TOF sequences were examined in BLASTp against *A.indica*protein database and obtained 5 sequences. The three-dimensional structures of five Neem proteins (Cytochrome P450, Cytochrome P450 (Partial), Squalene Epoxidase 1, Cytochrome f (Chloroplast), and Putative LOV Domain-Containing Protein) generated using SWISS-MODEL (Figure 1) proteins structure and functions (Table 1)and structures validations obtained by Ramachandran plots ofProcheck (Figure 2& Table 2) were given.

Figure 1 Modelled protein 3d structures of 1) CytochromeP450 2) CytochromeP450 3) Squalene epoxidase 1 4) Cytochrome f (chloroplast) 5) Putative LOV domain-containing protein.

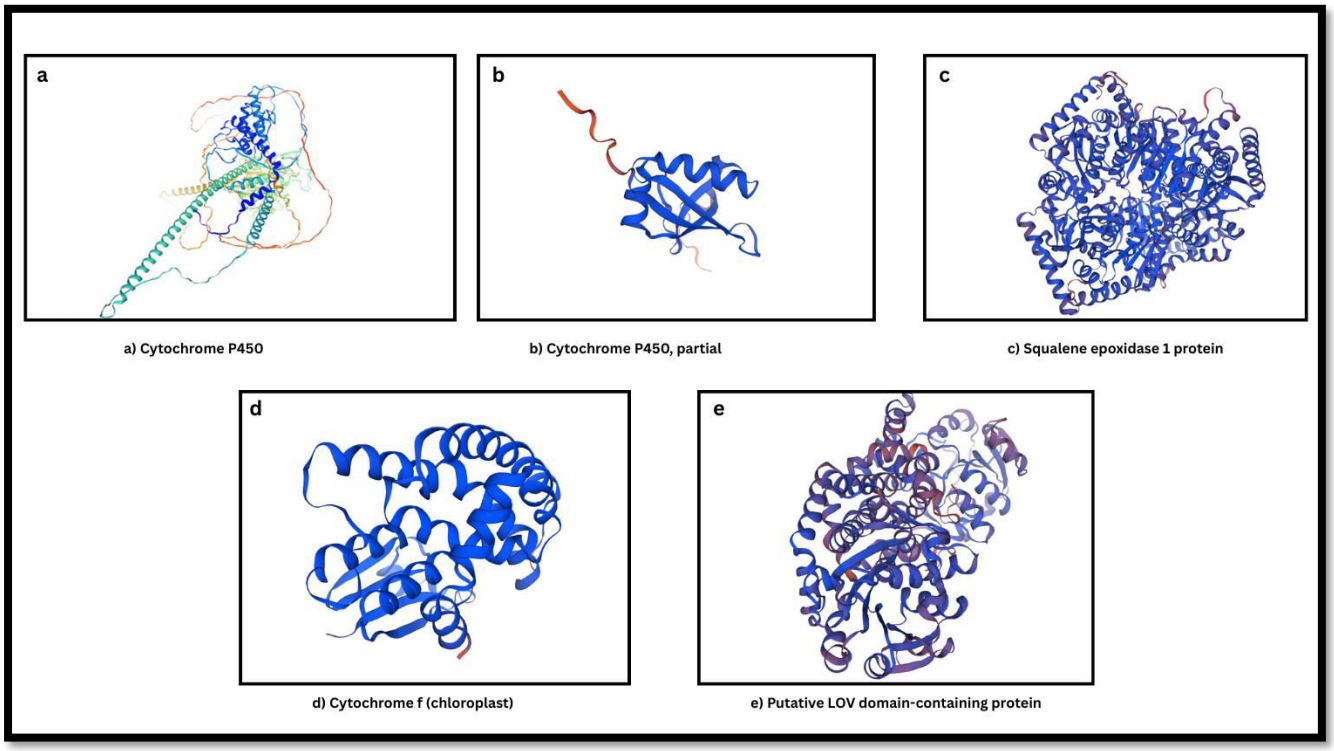

Table 1Neem Leaves Proteins including their source and Function

S. No.	Protein Name	Function/role	Modelled protein Structural observation
1.	Cytochrome P450	Heme-thiolatemonooxygenase; catalyzes oxidation reactions	It has a mixed structure with alpha helices along with beta sheets random coils which is a typical globular protein fold.
2.	Cytochrome P450 (Partial)	Fragmented isoform of the full length enzyme	It exhibits primarily alpha helices showing the characteristic right-handed spiral conformation of alpha helices.
3.	Squalene Epoxidase 1	Catalyzessqualene → 2,3-epoxysqualene; key in sterol biosynthesis	It has predominantly alpha helices throughout the structure, forming a complex globular protein with multiple

S. No.	Protein Name	Function/role	Modelled protein Structural observation
			helical domains.
4.	Cytochrome f (Chloroplast)	Electron transport in photosynthetic chain	It has a combination of alpha helices and beta sheet structures.
5.	Putative LOV Domain-Containing Protein	Light-sensing domain; often regulates transcription or enzymatic activity	It exhibits alpha helices spread within beta sheet structures.

Figure2 Ramachandran plots for five modelled Neem proteins, illustrating the distribution of backbone dihedral angles (φ and ψ) and stereochemical quality of each structure

1. Cytochrome P450 2. Cytochrome P450 partial 3. Squalene epoxidase 1
4. Cytochrome f (chloroplast) 5. Putative LOV domain-containing protein

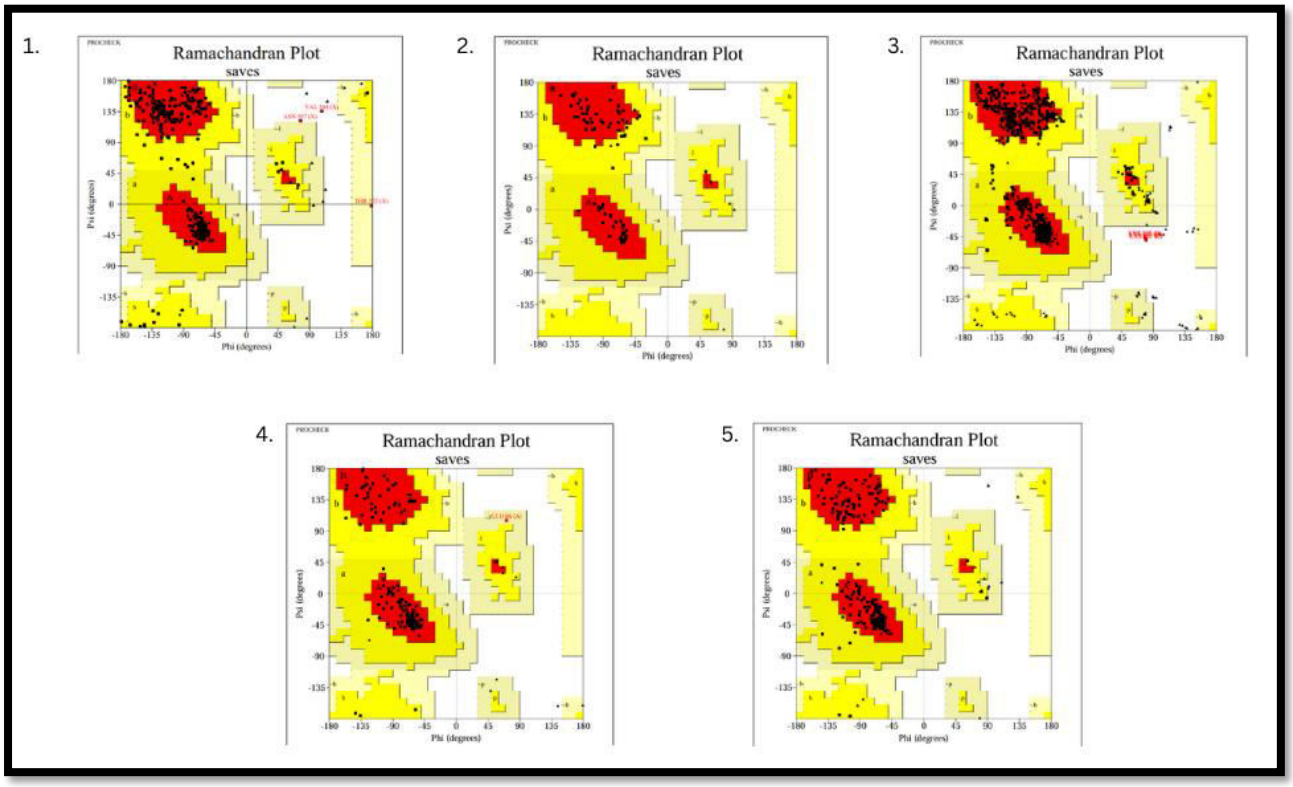

The stereochemical quality of the five modelled neem-derived proteins was evaluated using Ramachandran plot analysis generated by PROCHECK. The analysis revealed that **more than 94%** of the residues in Squalene Epoxidase 1,

Cytochrome f (chloroplast), and Putative LOV-domain containing protein occupied the most favored regions, indicating that these structures are highly stable and geometrically reliable. *Cytochrome P450 (full)* and *Cytochrome P450 (partial)* exhibited slightly lower percentages (88.9% and 85.2%, respectively), which remain acceptable for homology-modeled proteins, with minor deviations observed in flexible loop regions (Fig. 2) (Table 2).The absence of residues in disallowed regions (0.0–0.6%) across all proteins, along with minimal rotamer outliers (<1%) and low clash scores (2.8–3.4), indicates good backbone geometry and side-chain orientation. The RMSD values (1.2–2.0 Å) further confirm close alignment with template structures, reflecting overall model accuracy. These findings demonstrate that the generated neem protein models are structurally sound and suitable for docking studies against CDK and tubulin targets.

Table 2 Ramachandran Plot Metrics of Neem Proteins

Protein	**Most Favored (%)**	**Additional Allowed (%)**	**Disallowed (%)**	**Clash score**	**Rotamer Outliers (%)**	**RMSD (Å)**
Cytochrome P450	88.9%	10.2%	0.6%	2.8	0.4%	1.2
Cytochrome P450 partial	85.2%	14.8%	0.0%	3.2	0.5%	1.5
Squalene epoxidase 1	94.2%	5.4%	0.4%	2.9	0.3%	1.6
Cytochrome *f* (chloroplast)	95.7%	3.7%	0.0%	3.1	0.4%	1.8
Putative LOV domain-containing protein	95.1%	4.9%	0.0%	3.4	0.6%	2.0

Three-Dimensional Structures of Cancer targets:

Cyclin-dependent kinases (CDKs) and tubulin are both major therapeutic targets in cancer. Their sequences were retrieved from Protein Data Bank and the three-dimensional structures of the developed proteins are as follows.

A) **Cyclin-dependent kinases (CDKs) :** PDB of cyclin dependent kinases was retrieved from PDB database with accession number NP_001307847.1 (Sussman JL et al., 1998)

Figure 3 Three-Dimensional Structures of Cyclin-dependent kinases (CDKs)

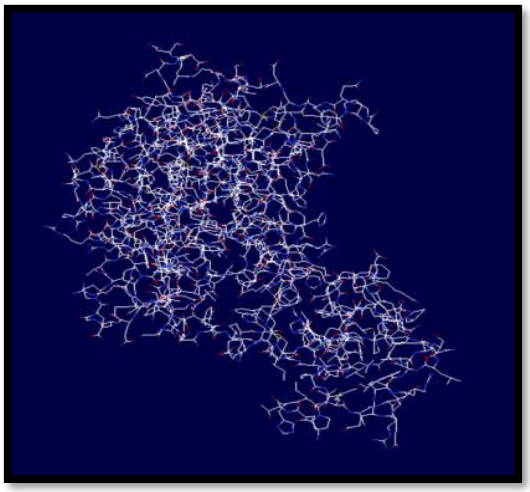

Cyclin-dependent kinases (CDKs)

B) **Tubulin :** PDB of Tubulin was retrieved from PDB database with accession number VDK36218.1 (Sussman JL et al., 1998)

Figure 4 Three-Dimensional Structures of Tubulin

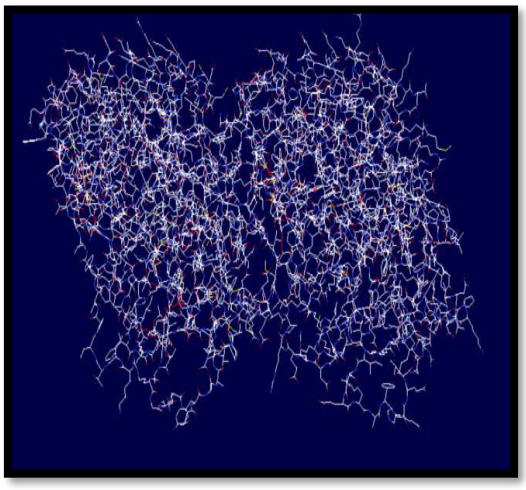

Tubulin

3.2 Molecular Docking of Neem proteins against the two cancer targets

Protein–protein docking using ZDOCK 3.0.2 revealed strong and biologically relevant interactions between Neem-derived proteins and the selected cancer targets such as Cyclin-dependent kinases (CDK) and Tubulin. Among all models, the Putative LOV-domain containing protein formed the largest interaction interface with CDK, engaging 43 amino acid residues and exhibiting a favourable force-field energy of −45,752.6, followed by Squalene Epoxidase 1 with 31 interacting residues and the most negative binding score (−69,219.0)(Fig. 6). Similarly, Cytochrome P450 demonstrated robust binding with Tubulin through 41 interacting residues, corresponding to an interaction energy of −51,616.0, suggesting high stability and strong affinity at the interface.Analysis of the binding interfaces revealed that the majority of contacts involved **charged and polar residues**. Notably, Asp, Glu, Lys, and Arg forming multiple hydrogen bonds and salt bridges that contribute to electrostatic stabilization. Additionally, **hydrophobic and aromatic residues** such as Ile, Leu, Phe, and Trp were distributed along the interface, implying significant van der Waals and π–π stacking interactions that enhance complex stability(Fig. 6). The high number of polar and nonpolar contacts indicates a complementary binding interface that could effectively modulate the target proteins' active or regulatory sites.From a functional standpoint, the interaction patterns suggest that *Putative LOV-domain containing protein* and *Squalene Epoxidase 1* could act as potent inhibitors of CDK activity by interfering with substrate or cyclin-binding regions, whereas Cytochrome P450 may destabilize microtubule dynamics through strong binding with tubulin. Docking analysis revealed that Squalene Epoxidase 1 interacts strongly with tubulin through a network of hydrophobic (ILE39, VAL31, PHE60, TYR66, LEU405), polar (ASN64, SER44, THR17, GLY71), and charged (GLU37, ASP34, LYS402) residues. The interface is dominated by van der Waals and π–π stacking interactions, supported by hydrogen bonds and electrostatic contacts, which collectively account for the high binding score (−53,204.012) and predict a stable SQE1–tubulin complex (Fig. 7).The other two proteins, Cytochrome P450 (partial) *and* Cytochrome f (chloroplast)*,* exhibited weaker interactions but still demonstrated measurable affinity, suggesting potential secondary or modulatory effects (Fig. 6,7).

Figure 6 Docking visualization between target and ligand

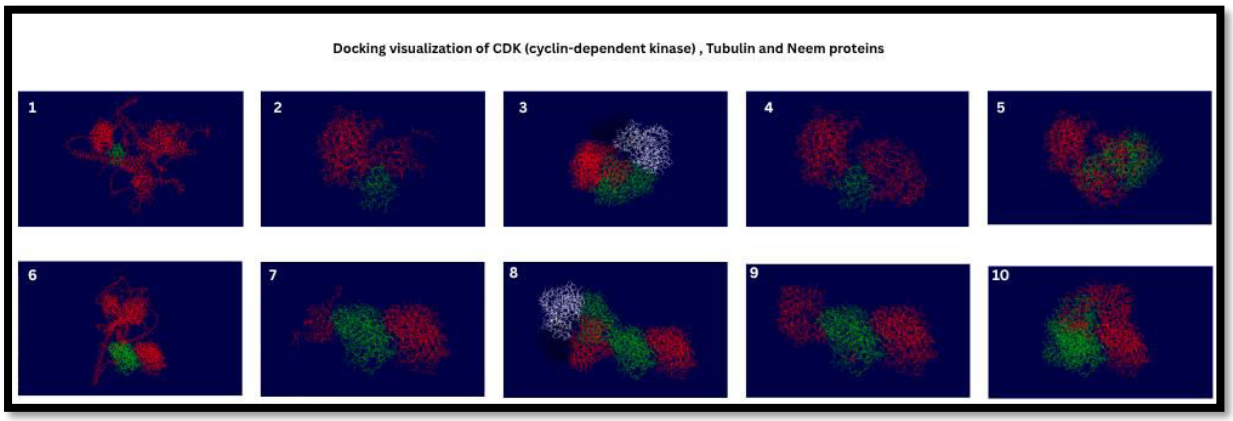

1. Docking visualization of CDK (cyclin-dependent kinase) and Cytochrome P450
2. Docking visualization of CDK (cyclin-dependent kinase) and Cytochrome P450 partial
3. Docking visualization of CDK (cyclin-dependent kinase) and Squalene epoxidase 1
4. Docking visualization of CDK (cyclin-dependent kinase) and Cytochrome *f* (chloroplast)
5. Docking visualization of CDK (cyclin-dependent kinase) and Putative LOV domain-containing protein
6. Docking visualization of Tubulin and Cytochrome P450
7. Docking visualization of Tubulin and Cytochrome P450 partial
8. Docking visualization of Tubulin and Squalene epoxidase 1
9. Docking visualization of Tubulin and Cytochrome *f* (chloroplast)
10. Docking visualization of Tubulin and Putative LOV domain-containing protein

3.4 Amino acids interactions of Neem proteins against CDK (cyclin-dependent kinase) and Tubulin:

Cytochrome P450, Squalene epoxidase 1, Putative LOV domain-containing proteinNeem proteins showed high interactions with CDK and Tubulin in contrast Cytochrome P450 partial, Cytochrome *f* (chloroplast)showed least interactions with CDK and Tubulin.

Figure 7 Amino acids interactions of Neem proteins against ligands

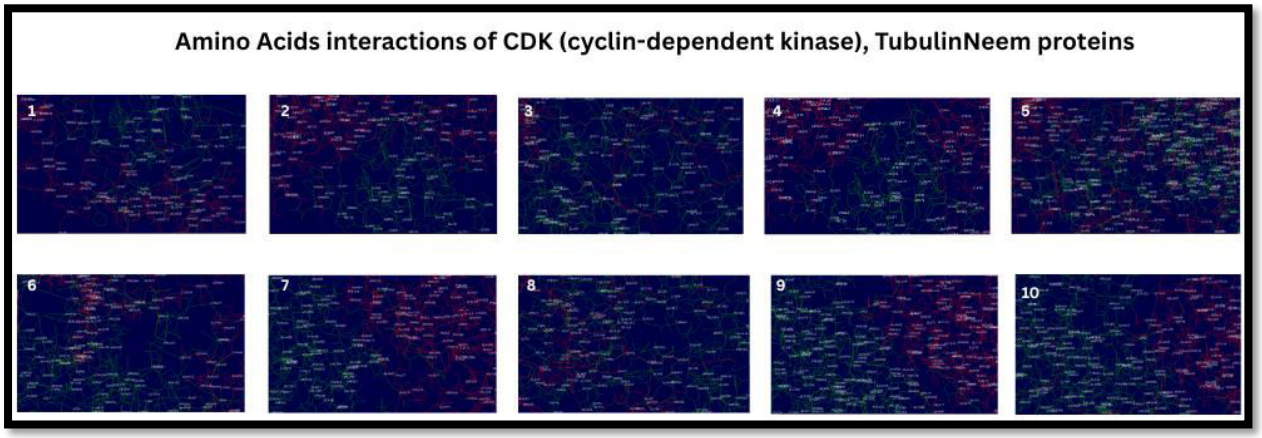

1. Amino acids interactions of CDK (cyclin-dependent kinase) and Cytochrome P450
2. Amino acids interactions of CDK (cyclin-dependent kinase) and Cytochrome P450 partial
3. Amino acids interactions of CDK (cyclin-dependent kinase) and Squalene epoxidase 1
4. Amino acids interactions of CDK (cyclin-dependent kinase) and Cytochrome *f* (chloroplast)
5. Amino acids interactions of CDK (cyclin-dependent kinase) and Putative LOV domain-containing protein
6. Amino acids interactions of Tubulin and Cytochrome P450
7. Amino acids interactions of Tubulin and Cytochrome P450 partial
8. Amino acids interactions of Tubulin and Squalene epoxidase 1
9. Amino acids interactions of Tubulin and Cytochrome *f* (chloroplast)
10. Amino acids interactions of Tubulin and Putative LOV domain-containing protein

Table 4 Core Amino acids interactions between Neem Proteins with Targets and theirForce field energy

Neem Protein	**Target**	**Core interacted Amino acids**	**Number of Amino acids Interacted**	**Force field energy**
Cytochrome P450	CDK	GLN283, PRO62, THR240, HIS36, THR35, GLU278, GLU7, LYS34, PRO276, PRO33, LYS356, VAL32, LEU271, TYR269, GLU270, ASN267, THR14, VAL48, TRP54, VAL55, ARG44, GLU42	**22**	**-51616.016**

Cytochrome P450 Partial	CDK	GLN61, PRO62, SER208, ASP207, ASP14, GLU15, PHE13, TYR12, VAL30, ALA38, THR12, SER29, PHE42, GLU46, TYR8, GLU45, ASP10, THR12	**18**	**-16739.021**
Squalene epoxidase 1	CDK	PRO40, ALA63, HIS205, VAL165, VAL17, GLY206, SER65, VAL164, ASP211, SER208, THR161, HIS162, PHE13, PRO25, ILE 66, ARG71, GLU101, SER230, ASN64, ILE107, LYS108, ASN64, TYR8, TYR7, GLN102, ILE39, ALA79, LEU136, CYS118, LYS132, VAL127	**31**	**-69219.070**
Cytochrome *f* (chloroplast)	CDK	ARG215, GLY206, ASP207, ASP14, PRO62, THR240, GLU61, GLU15, ASP207, ASP14, ASP10, LYS11, VAL77, ALA79, HIS76, LEU73, LEU87, SER51, GLN50, GLN88, GLN49, MET93	**22**	**-22907.775**
Putative LOV-domain containing protein	CDK	THR14, LYS34, GLN212, GLU15, ASP14, ASP211, HIS162, SER208, GLU209, PRO62, HIS60, SER52, GLU61, HIS21, VAL22, ARG20, GLU18, LEU73, TYR7, TYR8, TYR248, ALA115, ASN245, ALA322, SER25, LYS7, ILE250, ASP6, ARG175, MET324, LEU237, GLY144, TRP326, PRO132, LEU52, ALA106, LEU61, ALA99, HIS134, ASP236, LEU233, LYS232, ALA131	**43**	**-45752.625**
Cytochrome P450	Tubulin	ASN424, ILE788, GLU196, SER795, ASN767, ASN786, LYS796, GLU125, GLU797, ASN785, HIS704, ILE157, VAL790, ILE783, GLU782, LYS156, ARG273, GLU160, TYR867, GLU159, ARG868,	**41**	**-51616.016**

		ASP874, SER126, ARG123, LYS777, LYS124, GLU799, GLU732, VAL798, ILE783, ILE157, ASP874, TYR161, GLY410, ASP130, SER120, LEU132, TRP407, ARG253, VAL257, ALA256		
Cytochrome P450 Partial	Tubulin	GLN176, GLN247, ASN345, SER178, LEU248, PRO348, ALA400, ALA174, PRO173, ALA400, GTP500, ASP396	**12**	**-16739**
Squalene epoxidase 1	Tubulin	GLU37, GLY229, ILE39, ASN64, ALA63, ALA231, SER44, PHE232, GLY104, VAL31, GLU70, ILE105, VAL103, TYR66, MET32, GLY71, LYS5, ALA19, ALA72, THR17, ARG73, ALA114, GLY15, GLY16, TYR110, ALA69, GLU67, ILE47, PHE60, ILE39, ASN64, GLY88, GLY80, LYS402, LEU405, ASP414, ILE95, GLY80, GLU101, ASP34, THR228	**41**	**-53204.012**
Cytochrome *f* (chloroplast)	Tubulin	GLN247, GLY246, LEU248, SER178, ASN249, ARG2, HIS406, MET1, VAL409, GLY410, GTP500, THR73, VAL182, GLU183, LYS394, GLY81, ALA174, GLY142, LYS394, PRO173, SER178, LEU248, PRO348, ALA180	**24**	**-50016.010**
Putative LOV-domain containing protein	Tubulin	SER70, PHE167, ALA421, GLN193, ALA57, GLN136, THR108, TYR202, ILE384, SER301, ARG243, VAL344, ARG2, HIS406, TRP407, MET1, ASP98, TYR408, ASN249, PRO348, THR73, PRO173, ASN50, TYR292, THR317, VAL182, LYS254, ASP251, ARG2	**29**	**-67190.050**

Energy calculation and Energy interpretation

The current study, showed that the Putative LOV Domain-Containing Protein, Squalene Epoxidase 1, and Cytochrome P450 displayed the most favorable energy profiles, with binding energies of −45,752.6 kJ/mol, −69,219.0 kJ/mol, and −51,616.0 kJ/mol, respectively. These low energy values indicate strong and stable protein–protein associations with both CDK and tubulin.The distribution of energy components revealed that electrostatic interactions and hydrogen bonding were dominant stabilizing forces, while van der Waals contributions supported interface complementarity. Complexes with minimal RMSD deviations (1.2–2.0 Å) and low clash scores exhibited the highest structural stability.Overall, energy analysis confirmed that the Neem-derived proteins, particularly the Putative LOV Domain-Containing Protein, Squalene Epoxidase 1, and Cytochrome P450, form energetically favorable and biologically plausible interactions with cancer targets, supporting their potential as effective anticancer modulators.

Visualization and Interaction Mapping

The binding energy values and the number of interacting residues were extracted for each complex, and interface residues forming hydrogen bonds or electrostatic interactions were catalogued for both CDK and tubulin targets. The Putative LOV Domain-Containing Protein, Squalene Epoxidase 1, and Cytochrome P450 demonstrated the most extensive interaction networks, with residues such as THR14, LYS34, GLU15, HIS162, SER208, TYR7, TYR248, ARG71, GLU101, and TYR867showing strong binding complementary. The **electrostatic surface potential** of each receptor and ligand was calculated to evaluate charge complementary at the binding site, while solvent-accessible surface areas (SASA) were analyzed to understand the extent of interface burial upon complex formation. The Ramachandran plot data, rotamer conformations, and clash scores of interacting residues were revalidated to ensure stereochemical accuracy of the final docked models.Three-dimensional visualizations were rendered to depict the binding pocket topology, interactiondistances, and interface geometry of each complex. The results from these analyses provided crucial insights into the molecular determinants governing Neem protein interactions with CDK and tubulin, forming the basis for subsequent structural interpretation and functional correlation.

Discussion:

Plant-derived peptides have emerged as promising bioactive molecules with significant anticancer potential. These small, naturally occurring proteins can selectively target cancer cells, induce apoptosis, inhibit angiogenesis, and block tumor progression while causing minimal harm to normal cells. Neem peptides, in particular, have drawn attention for their strong antioxidant and cytotoxic activities. Studies suggest that neem-derived proteins and peptides can interfere with critical cancer pathways, such as those involving tubulin dynamics and cell-

cycle regulation through cyclin-dependent kinases (CDKs). Their natural origin, structural stability, and low toxicity make neem peptides valuable leads for developing safer, more effective anticancer therapeutics. Neem has antioxidant, anti-inflammatory and anticancer effects with compounds e.g., nimbolide, azadirachtin and various triterpenoids/limonoids (Hao et al., 2014). In our earlier (Al Saiqali et al., 2024) and current study we identified five neem proteins Cytochrome P450, Cytochrome P450 (partial), Squalene Epoxidase 1 (SQE1), Cytochrome f (chloroplast), and a Putative LOV (light–oxygen–voltage) domain by LC-MS.Study conducted by Agrawalal.,(2020) reveals the anticancer properties of neemethanolic leaf extracts, neem leaf glycoprotein, liminoids like Azadirachtin and Nimbolide. Which were demonstrated to unequivocally have preventive and therapeutic potential against oral cancer were in the present study, extracted neem proteins was interacted effectively with the cancer targets i.e CDK and Tubulin.

Madeswaran et al.,(2024) studyformulated a nanosuspension with curcumin and nimbin and assessed its anticancer potential using *in silico* molecular docking and *in vitro* MTT assay for colorectal cancer. The docking studies were conducted using AutoDock 4.2.The BIOVIA Discovery studio visualizer tool was used to display the binding orientations. In present study neem proteins (Cytochrome P450 (full and partial), Squalene Epoxidase 1, Cytochrome f and Putative LOV Domain-Containing Protein) was isolated, analyzed by SDS-PAGE, sequenced via MALDI TOF/TOF, and its 3D models generated using SWISS-MODEL. The docking studies against cancer targets were conducted by using Zdock 3.0.2 version. The Spdbv viewer was used to view the target and ligand interactions (Agboola et al., 2025).

Cytochrome P450 (CYP) superfamily are heavily involved in secondary metabolism (oxidative tailoring of terpenoids and other natural products). CYPs or their catalytic products are plausible indirect sources of anticancer molecules (Bhambhani et al., 2017).CYP enzymes also play a role in the bioactivation of prodrugs (Rendic et al., 2021). Prodrug therapy (GDEPT) in cancer therapy is achieved by delivering enzymes (e.g., CYP) ideally directly to targeted tumor cells where non-toxic chemotherapy prodrugs are transformed by the CYP into their cytotoxic form to cause cancer cells death(Chen e al., 200).Second, squaleneepoxidase (SQE/SQE1) catalyses a committed oxidation step in triterpenoid and sterol pathways (Pandreka et al., 2015).

Tubulin (and the dynamic microtubule system) and CDKs are canonical anticancer targets. Microtubule-targeting agents disrupt mitosis and remain frontline chemotherapeutics, while CDKs control the cell-cycle transitions and transcriptional programmes that are frequently deranged in cancer; selective CDK inhibitors are clinically validated (e.g., CDK4/6 inhibitors) and multiple CDK families are attractive therapeutic targets. Targeting either pathway can arrest proliferation and promote cancer cell death, making them suitable endpoints for in silico screens (Cheng et al., 2020). Our study predicted that neem protein could

bonded strongly with tubulin leading to destabilize microtubules.Tubulin inhibitors and biological agents have entered clinical trials. For example, rilotumab and erlotinib were used in combination to treat patients with lung cancer. These results are in accordance with this study findings were cytochrome P450 were found to bind strongly with Tubulin (Cheng et al., 2020; Tarhini et al., 2017).

A polypeptide based PPT conjugate PLG-g-mPEG-PPT was and used for the treatment of multi drug resistant breast cancer. The PLG-g-mPEG-PPT was prepared by conjugating PPT to poly(l-glutamic acid)-g-methoxy poly(ethylene glycol) (PLG-g-mPEG) via ester bonds (Zhou et al., 2018).This result in correlation with our finding where our peptides showed excellent anticancer activities against two main anticancer targets CDK and tubulin. Neem extracts have been reported to show relative selectivity for cancer versus normal cells in multiple studies. Computationally, selectivity can be anticipated by comparing predicted binding energies across a panel of human off-targets and by evaluating predicted ADMET properties of peptides (Hao et al., 2014).

In the similar line Khalid et al., (2024)evaluated the anticancer effects of a methanol extract ofNeem on a human hepatocellular carcinoma cell line (HepG2) using an in vitro MTT assay and by insilico approachto investigate the interaction between neem and Akt1, a protein kinase implicated in the pathogenesis of hepatocellular carcinoma (HCC) via the PI3K/Akt/mTOR pathway. His study identified two promising Akt1 inhibitors, 2′,3′-dehydrosalannol and quercetin, with improved binding affinity and a safe pharmacological profile. In our findings we have identified three promising CDK and tubulin inhibitors namely (Cytochrome P450, Squalene epoxidase 1, Putative LOV-domain containing protein).

Conclusion:

It is driving the development of more precise and less harmful cancer treatments. The advances are enabling targeted therapies that spare healthy tissue, accelerating the shift toward personalized, patient-focused oncology care. This in silico study provides compelling evidence that Neem (Azadirachtaindica) derived proteins possess significant potential as natural anticancer agents targeting two key regulatory proteins such as Cyclin-Dependent Kinases (CDKs) and tubulin. Among the five modeled Neem proteins, the Putative LOV Domain-Containing Protein, Squalene Epoxidase 1, and Cytochrome P450 demonstrated the most favorable binding energies and extensive amino acid interactions, indicating strong and stable complex formation with both cancer targets. The low RMSD values (1.2–2.0 Å) and minimal steric clashes confirm the high structural reliability of the modeled complexes, reinforcing the accuracy of the docking results. Collectively, these findings reveal that Neem-derived proteins, particularly the Putative LOV Domain-Containing Protein, Squalene Epoxidase 1, and Cytochrome P450, could serve as promising dual-action modulators of CDK

and tubulin. Future directions should include biochemical validation and cellular assays to confirm these interactions experimentally, along with structure–activity relationship (SAR) and molecular dynamics simulations to refine their therapeutic potential. This integrative approach bridges computational modeling with plant-based drug discovery, highlighting Neem's vast potential as a sustainable source of next-generation anticancer therapeutics.

References:

1. Mookherjee N, Anderson MA, Haagsman HP, Davidson DJ. Antimicrobial host defence peptides: functions and clinical potential. Nat Rev Drug Discov. 2020;19(5):311–32.
2. Roudi R, Syn NL, Roudbary M. Antimicrobial peptides as biologic and immunotherapeutic agents against cancer: a comprehensive overview. Front Immunol. 2017;8:1320.
3. Zhang LJ, Gallo RL. Antimicrobial peptides. Curr Biol. 2016;26(1):R14–9.
4. Pfalzgraff A, Brandenburg K, Weindl G. Antimicrobial peptides and their therapeutic potential for bacterial skin infections and wounds. Front Pharmacol. 2018;9:281.
5. Hoskin, D. W., & Ramamoorthy, A. (2008). Studies on anticancer activities of antimicrobial peptides. Biochimica et BiophysicaActa (BBA) - Biomembranes, 1778(2), 357–375.
6. Hancock, R. E. W., Alford, M. A., & Haney, E. F. (2021). Anticancer peptides: Broad-spectrum agents for cancer therapy. Trends in Cancer, 7(9), 682–694.
7. Hao, Fang, et al. "Neem components as potential agents for cancer prevention and treatment." Biochimicaet Biophysica Acta (BBA)-Reviews on Cancer 1846.1 (2014): 247-257.
8. Ray, S. et al. (2022) 'Antibacterial and antifungal activities of Azadirachtaindica A. Juss (Neem): A review', Modern Approaches in Chemical and Biological Sciences.
9. Mohideen, M. et al. (2022) 'An overview of antibacterial and antifungal effects of Azadirachtaindica crude extract: a narrative review'
10. Al Saiqali, M., Tangutur, A.D. and Bhukya, B. (2021) 'Peptides and low molecular weight polypeptides of Azadirachtaindica seeds as new weapons against cancer cells and superbugs', Phytomedicine Plus, Vol.1, No.4, p.100118.
11. Rout, SK., Kar GBA, Mishra D. (2024) 'Evaluation of Anthelmintic Activity of Different Extracts of Azadirachtaindica Flower/Buds in Indian Earthworm', Acta Scientific Pharmaceutical Sciences 8.6: 28-33.
12. Bray F., Ferlay J., Soerjomataram I., Siegel R.L., Torre L.A., Jemal A. Global cancer statistics 2018: GLOBOCAN estimates of incidence and mortality worldwide for 36 cancers in 185 countries. CA Cancer J. Clin. 2018;68:394–424.

13. Boyle P., Levin B. World Cancer Report 2008. The International Agency for Research on Cancer; Lyon, France: 2008. pp. 12–510. WHO report.
14. Patrick G.L. An Introduction to Medicinal Chemistry. Oxford University Press; Oxford, UK: 2013.
15. Hawash M. Highlights on Specific Biological Targets; Cyclin-Dependent Kinases, Epidermal Growth Factor Receptors, Ras Protein, and Cancer Stem Cells in Anticancer Drug Development. Drug Res. 2019;69:471–478.
16. Singh H., Kumar M., Nepali K., Gupta M.K., Saxena A.K., Sharma S., Bedi P.M.S. Triazole tethered C5-curcuminoid-coumarin based molecular hybrids as novel antitubulin agents: Design, synthesis, biological investigation and docking studies. Eur. J. Med. Chem. 2016;116:102–115.
17. Helal, Christopher J., et al. "Discovery and SAR of 2-aminothiazole inhibitors of cyclin-dependent kinase 5/p25 as a potential treatment for Alzheimer's disease." Bioorganic & medicinal chemistry letters 14.22 (2004): 5521-5525.
18. Soni, Rajeev, et al. "Inhibition of cyclin-dependent kinase 4 (Cdk4) by fascaplysin, a marine natural product." Biochemical and biophysical research communications 275.3 (2000): 877-884.
19. Hörmann, Aldo, Bhabatosh Chaudhuri, and Heinz Fretz. "DNA binding properties of the marine sponge pigment fascaplysin." Bioorganic & medicinal chemistry 9.4 (2001): 917-921.
20. Jenkins, Paul R., et al. "Design, synthesis and biological evaluation of new tryptamine and tetrahydro-β-carboline-based selective inhibitors of CDK4." Bioorganic & medicinal chemistry 16.16 (2008): 7728-7739.
21. Varinska, Lenka, et al. "Angiomodulators in cancer therapy: New perspectives." Biomedicine & Pharmacotherapy 89 (2017): 578-590.
22. Pierce BG, Wiehe K, Hwang H, Kim BH, Vreven T, Weng Z. ZDOCK server: interactive docking prediction of protein–protein complexes and symmetric multimers. Bioinformatics. 2014 Jun 15;30(12):1771-3.
23. Mitternacht S. FreeSASA: An open source C library for solvent accessible surface area calculations. F1000Research. 2016 Feb 18;5:189.
24. Sussman JL, Lin D, Jiang J, Manning NO, Prilusky J, Ritter O, Abola EE. Protein Data Bank (PDB): database of three-dimensional structural information of biological macromolecules. Biological Crystallography. 1998 Nov 1;54(6):1078-84.
25. Senadheera, T.R., Hossain, A., Dave, D. and Shahidi, F., 2022. In silico analysis of bioactive peptides produced from underutilized sea cucumber by-products—A bioinformatics approach. Marine Drugs, 20(10), p.610.
26. Agrawal, S., Popli, D. B., Sircar, K., & Chowdhry, A. (2020). A review of the anticancer activity of Azadirachtaindica (Neem) in oral cancer. Journal of Oral Biology and Craniofacial Research, 10(2), 206.
27. Madeswaran, Arumugam, Selvam Tamilazhagan, and Sellappan Mohan. "In silico evaluation, characterization, and in vitro anticancer activity of

curcumin–nimbin loaded nanoformulation in HCT-116 cell lines." BioTechnologia 105.4 (2024): 355.

28. Agboola, Oluwaseun E., et al. "Integrative Genomic and in Silico Analysis Reveals Mitochondrially Encoded Cytochrome C Oxidase III (MT—CO3) Overexpression and Potential Neem-Derived Inhibitors in Breast Cancer." Genes 16.5 (2025): 546.
29. Bhambhani, S., Lakhwani, D., Gupta, P., Pandey, A., Dhar, Y. V., Kumar Bag, S., Asif, M. H., & Kumar Trivedi, P. (2017). Transcriptome and metabolite analyses in Azadirachtaindica: Identification of genes involved in biosynthesis of bioactive triterpenoids. Scientific Reports, 7(1), 1-12.
30. Rendic, S. P., and Guengerich, F. P. (2021). Human Family 1-4 cytochrome P450 enzymes involved in the metabolic activation of xenobiotic and physiological chemicals: an update. Arch. Toxicol. 95, 395–472.
31. Chen L., Waxman D. J. (2002). Cytochrome P450 gene-directed enzyme prodrug therapy (GDEPT) for cancer. Curr. Pharm. Des. 8
32. Pandreka, A., Dandekar, D. S., Haldar, S., Uttara, V., Vijayshree, S. G., Mulani, F. A., Aarthy, T., &Thulasiram, H. V. (2015). Triterpenoid profiling and functional characterization of the initial genes involved in isoprenoid biosynthesis in neem (Azadirachtaindica). BMC Plant Biology, 15, 214.
33. Cheng, Z., Lu, X., & Feng, B. (2020). A review of research progress of antitumor drugs based on tubulin targets. Translational Cancer Research, 9(6), 4020.
34. Tarhini AA, Rafique I, Floros T, et al. Phase 1/2 study of rilotumumab (AMG 102), a hepatocyte growth factor inhibitor, and erlotinib in patients with advanced nonsmall cell lung cancer. Cancer. 2017;123:2936-44.
35. Zhou H, Lv S, Zhang D, et al. A polypeptide based podophyllotoxin conjugate for the treatment of multi drug resistant breast cancer with enhanced efficiency and minimal toxicity. ActaBiomater2018;73
36. Khalid, H., Shityakov, S., Förster, C. Y., & Song, Y. (2024). Exploring the anticancer properties of Azadirachtaindica: In silico and in vitro study of its phytochemicals against hepatocellular carcinoma. Journal of Molecular Structure, 1317, 138962